Author Manuscript

Author Manuscript

Author Manuscript

Author Manuscript

HHS Public Access

Author manuscript

J Biomed Nanotechnol. Author manuscript; available in PMC 2017 March 09.

Published in final edited form as:

J Biomed Nanotechnol. 2015 December ; 11(12): 2197–2210.

Negatively Charged Carbon Nanohorn Supported Cationic Liposome Nanoparticles: A Novel Delivery Vehicle for Anti-Nicotine Vaccine

Hong Zheng[1,†], **Yun Hu**[1,†], **Wei Huang**[1], **Sabina de Villiers**[2,3], **Paul Pentel**[2], **Jianfei Zhang**[4], **Harry Dorn**[4], **Marion Ehrich**[5], and **Chenming Zhang**[1,*]

[1]Department of Biological Systems Engineering, Virginia Tech, Blacksburg, VA 24061, USA

[2]Minneapolis Medical Research Foundation, Minneapolis, MN 55404, USA

[3]Department of Physiology and Pharmacology, Karolinska Institute, Stockholm, Sweden

[4]Department of Chemistry, Virginia Tech, Blacksburg, VA 24061, USA

[5]Department of Biomedical Sciences and Pathobiology, Virginia Tech, Blacksburg, VA 24061, USA

Abstract

Tobacco addiction is the second-leading cause of death in the world. Due to the nature of nicotine (a small molecule), finding ways to combat nicotine's deleterious effects has been a constant challenge to the society and the medical field. In the present work, a novel anti-nicotine vaccine based on nanohorn supported liposome nanoparticles (NsL NPs) was developed. The nano-vaccine was constructed by using negatively charged carbon nanohorns as a scaffold for the assembly of cationic liposomes, which allow the conjugation of hapten conjugated carrier proteins. The assembled bio-nanoparticles are stable. Mice were immunized subcutaneously with the nano-vaccine, which induced high titer and high affinity of nicotine specific antibodies in mice. Furthermore, no evidence of clinical signs or systemic toxicity followed multiple administrations of NsL-based anti-nicotine vaccine. These results suggest that NsL-based anti-nicotine vaccine is a promising candidate in treating nicotine dependence and could have potential to significantly contribute to smoking cessation.

Keywords

Nicotine; Nicotine Vaccine; Anti-Nicotine; Bionanoparticle; Carbon Nanohorn; Nano-Vaccine

INTRODUCTION

Tobacco addiction is the second-leading cause of death in the world.[1, 2] How to help smokers to quit smoking has been a constant challenge to medical scientists. To date, three medications are FDA-approved for smoking cessation: nicotine replacement therapy,

*Author to whom correspondence should be addressed. Chzhang2@vt.edu.

†These two authors contributed equally to this work.

Author Manuscript Author Manuscript Author Manuscript Author Manuscript

sustained- release bupropion, and varenicline.[3, 4] Despite the relative efficacy of these first-line medications, long-term abstinence rates remain disappointingly low.[5] Clearly, more effective treatment options are needed. Immunopharmacotherapy, or vaccination, has shown tremendous promise in fighting against nicotine addiction.[6] Nicotine vaccines have the following advantages: (1) vaccines can have a prolonged effect on the immune system (6–12 months), and could thus reduce the relapse rates, (2) daily administration is not required; only occasional booster shots are needed to maintain an adequate antibody titer, (3) vaccines have minimal to no side effects, and (4) vaccines are potentially compatible with other smoking cessation methods. However, all current nicotine vaccines, particularly the ones that have undergone human clinical trials, demonstrated limited efficacy.[6–8] The recently released clinical trial results of NicVax® by Nabi Biopharmaceuticals were particularly disappointing.[9] On the other hand, a recent report described a successful trial in mice treated with adeno-associated virus (AAV) vector expressing a gene encoding a full-length anti-nicotine antibody.[10] However, it is still unclear how this success can be translated to humans, and the long-term safety of the system is still a significant obstacle. Because the success of drug vaccines appears to be directly correlated with the antibody titer in vaccinated subjects,[6–10] there is a need for improved vaccines that can elicit a strong immune response.

Over the past decade, particulate carriers have emerged as an attractive means for enhancing the delivery efficacy and potency of vaccines and associated immunomodulatory molecules. Specifically, polymer-based micro and nanoparticles are being extensively studied for this purpose. Polymeric micro and nanoparticles can carry cargo, whether antigens, adjuvants or both, either encapsulated within the particle or on the surface of the particle. They provide an efficient means for delivering antigen to antigen presenting cells (APCs), either in a passive manner through non-specific phagocytosis or in a more active manner through receptor targeting and endocytosis. The latter can be achieved by modifying the particle surface with antibodies against surface receptors of specific APC subsets e.g., DEC205 attachment for targeting to epidermal Langerhans cells.[11]

In addition to the particulate nanoparticles, proteins and peptides have demonstrated potential for being effective vaccine carriers. Protein derived particulate systems are biocompatible and degraded into natural byproducts, and they can be easily modified due to the large repertoire of amino acids with a variety of physical-chemical properties. Peptide/protein- based particles made of amino acids,[12] denatured collagen (gelatin),[13] and albumin[14] have been shown to be effective in eliciting immune responses. Moreover, liposomes, particulate structures composed largely of natural or synthetic phospholipids, can encapsulate both antigenic and immunomodulatory agents,[15–18] allowing targeted delivery to specific immune cells such as dendritic cells *in vivo*. Depending on their lipid composition, liposomes also may exhibit potent adjuvant-like properties.[19, 20] However, one of the main limitations of liposomes is that they are intrinsically unstable and often have a tendency to flocculate.[21]

In this study, novel negatively charged (anionic) carbon single-walled nanohorns (SWNHs) were used as a scaffold, providing support to the soft body of cationic liposomes. This support prevented the liposomes from precipitation or flocculation. The SWNHs are nontoxic[22, 23] nanoparticle aggregates of single graphene tubules and are spherical dahlia-

Author Manuscript Author Manuscript Author Manuscript Author Manuscript

like-shaped with a narrow diameter range reported as 80–100 nm.[24] For this study, nanohorns with a diameter of around 100 nm were encapsulated into liposomes through a simple freeze-thaw method as described in our previous work.[25] The nanohorn supported liposome nanoparticles (NsL NPs) were used as a vaccine delivery vehicle. The hapten derivative, O-succinyl-3′-hydroxmethyl-(±) nicotine (Nic), was used as the immunogen.[26] The immunogenicity and toxicity of the nano-vaccines were studied in mice.

MATERIALS AND METHODS

Materials

All chemicals were obtained from Sigma-Aldrich (St. Louis, MO, USA) unless otherwise noted. 1,2-dioleoyl-3-trimethylammonium-propane (DOTAP) and 1,2-distearoyl-sn-glycero-3-phosphoethanolamine-*N*-[maleimide(polyethylene glycol)-2000] (ammonium salt) (DSPE-PEG(2000)-maleimide) were purchased from Avanti Polar Lipids (Alabaster, AL, USA). EDC (1-ethyl-3-[3-dimethylaminopropyl] carbodiimide) was obtained from Pierce (Rockford, IL, USA). O-succinyl-3′-hydroxmethyl-(±) nicotine (nicotine hapten) was purchased from Toronto Research Chemicals (Toronto, ON, Canada).

Preparation of Nanohorn Supported Liposome Nanoparticles (NsL)

NsL NPs were prepared according to the method described by Huang et al.[25] Briefly, cationic liposomes were made by extruding 1.96 mg hydrated DOTAP and 0.32 mg DSPE-PEG(2000)-maleimide lipid film through polycarbonate membranes with pore sizes of 100 nm. The hydration buffer contained 0.9% NaCl, 5% dextrose, and 10% sucrose in Tris-HCl buffer with pH at 7.4. Single-walled nanohorns (SWNH) were synthesized by Nd:YAG laser vaporization of graphite rods in an argon atmosphere at 1100 °C.[27, 28] Negatively charged (anionic) nanohorns with carboxyl groups were prepared by high-speed vibration milling.[29] Anionic nanohorns were briefly sonicated to break up aggregates and incubated with freshly made cationic liposomes at a volume ratio of 1:4. Three freeze-and-thaw cycles were applied using −80 °C and a warm water bath (30 °C). Samples were finally centrifuged under 10,000 ×*g* for 10 min, and nanohorn supported liposomes were collected from the top layer of the solution.

Synthesis and Quantification of Nic-BSA Conjugates

The synthesis of Nic-BSA conjugates was based on the procedure described elsewhere.[30] Briefly, a solution of 1-ethyl-3-(3-dimethylaminopropyl) carbodiimide (EDC, 10 molar equivalents compared to nicotine hapten) in distilled H_2O was added to 10 mg nicotine hapten water solution (100 mg/mL) and kept at 0 °C for 10 min. The solution was then mixed with 10 mg bovine serum albumin (BSA) solution (40 mg/mL) and an appropriate amount of distilled water to prepare a total volume of 1 mL. The solution was stirred at 0 °C for 10 min, and stored at room temperature overnight. During this step, pH was checked and adjusted to 6.76 with 0.01 M sodium hydroxide if needed. Nic-BSA conjugates were purified by size exclusion chromatography with a Sephadex G-25 column using an AKTA FPLC system (GE Healthcare, Piscataway, NJ). Nic-BSA was then concentrated to 1 mg/mL using Microcon centrifugal filter units (EMD Millipore Corporation, Billerica, MA) with a 50,000 molecular weight cut-off (MWCO). The number of -NH_2 groups used during

Author Manuscript Author Manuscript Author Manuscript Author Manuscript

conjugation of hapten to BSA molecules was determined from the difference between the optical density of the control and the conjugate by a method utilizing 2,4,6-trinitrobenzene-1-sulfonic acid (TNBS).[31]

Thiolation of Nic-BSA Conjugates

Thiol groups were introduced to Nic-BSA by incubating Nic-BSA obtained in the previous step with 1 mg/mL of 2-iminothiolane (Traut's reagent) for one hour in darkness under continuous stirring.[32] The thiolated Nic-BSA was purified using FPLC as described for Nic-BSA purification and concentrated to 2 mg/mL in phosphate buffered saline (PBS, pH 7.4) by Microcon centrifugal filter units (50,000 MWCO). The amount of thiol groups on BSA was quantified by a colorimetric sulfhydryl assay using Ellman's reagent (5,5′-dithiobis(2-nitrobenzoic acid).[33] Briefly, Ellman's reagent (80 μL of a 4 mg/mL solution in PBS) was added to 0.6 mL aliquots of a control and the samples and allowed to incubate at room temperature for 20 min. Sulfhydryl levels were determined from the absorbance at 412 nm (ε = 14398) using the equation,

$$\mathrm{SH}=1.1\mathrm{A}_{412}/14398\mathrm{C}_{\mathrm{Nic-BSA}}$$

where A_{412} is the absorbance at 412 nm, CNic-BSA is the protein concentration, and SH is the number of thiol equivalents.

Conjugation of Thiolated Nic-BSA to NsL

The thiolated Nic-BSA was mixed with the maleimide-PEG–containing nanohorn supported liposomes in 0.15 M NaCl, 0.2 mM EDTA (pH 7.4) at a molar ratio of 1:8 and allowed to react overnight. Unbound protein was separated from the liposomes by dialysis using dialysis membrane (MWCO 1000 kD) from Spectrum Laboratories in 0.15 M NaCl pH 7.4 solution. Nic-BSA associated with liposomes was assayed using a modified protocol described by Ansell.[34] Briefly, 20 μL of prepared liposomes (before and after purification) were diluted with 1 mL 0.15 M NaCl pH 7.4 solution (working dispersion). To assess the total and conjugated protein concentration, 500 μL of working dispersion were mixed with 100 μL of 5% (v/v) Triton X-100, and this mixture was maintained at 65 °C for 5 min to disrupt all lipid vesicles. Both total and conjugated Nic-BSA concentrations were measured using a micro BCA protein assay kit from Pierce (Rockford, IL). The association efficiency (AE) and the loading capacity (LC) of Nic-BSA to nanohorn supported liposomes were calculated according to the following equations:

$$\mathrm{AE}(\%)=\mathrm{Nic}-\mathrm{BSA}_{\mathrm{conjugated}}/\mathrm{Nic}-\mathrm{BSA}_{\mathrm{Total}}\times 100\%$$
$$\mathrm{LC}(\%)=\mathrm{Nic}-\mathrm{BSA}_{\mathrm{conjugated}}/\mathrm{NPs}\times 100\%$$

Characterization of NPs

Dynamic Light Scattering (DLS) and Zeta-Potential—Particle sizes and distribution of the nanohorn, liposomes, NsL and Nic-BSA-NsL were measured by photon correlation spectroscopy (PCS) using a Zetasizer Nano (Malvern Instruments, UK). Prior to the DLS measurement, each sample was diluted with 0.15 M NaCl pH 7.4 solution until a measurable

Author Manuscript Author Manuscript Author Manuscript Author Manuscript

concentration of particles was achieved. Similarly, the zeta potential of the samples was measured using the same equipment with Laser Doppler Velocimetry.[35] Both measurements were repeated three times for each sample.

Transmission Electron Microscopy (TEM)—Sample grids (carbon coated copper) were put into one drop of liposomes for 30 s, then in a distilled water drop for washing (10 s) and finally in a phosphotungstic acid drop for staining (10 s).[36] The excessive stain on the grids was removed using filter paper. The prepared grids were analyzed using a Morgagni™ Transmission Electron Microscope (FEI Corporate, Hillsboro, OR).

Stability of NsL NPs—Stability was monitored using imaging of fluorescent dyes encapsulated following a published method.[37] Briefly, lipid films containing 1.96 mg 1,2-dioleoyl-3-trimethylammonium-propane (DOTAP) and 0.2 mg fluorescein isothiocyanate (FITC) isomer I (molar ratio, 100:2) were hydrated with 250 μL of hydration buffer (Section 2.2). The resulting emulsion was incubated at 65 °C for one hour and extruded 14 times through polycarbonate membranes with pore sizes of 100 nm. For nanohorn supported liposomes, the FITC labeled liposomes underwent 5 cycles of freeze-and-thaw at −80 °C and 35 °C when 62.5 μL of a nanohorn solution (1 mg/mL) were added. The resulting mixture was centrifuged at 16,000 × *g* for 30 min, and the nanohorn supported liposomes were collected from the top layer of the solution. Excessive FITC in both liposomes and nanohorn liposomes was removed by 24 h of dialysis using 100 kD Biotech CE Dialysis Tubing (Spectrum Laboratories, Inc., Rancho Dominguez, CA, USA) in distilled water. Morphology was viewed on a LSM510 confocal laser scanning microscope (Carl Zeiss Inc, Thornwood, NY, USA).

Vaccination

Immunization Procedures—All animal studies were carried out following the National Institutes of Health (NIH) guidelines for animal care and use. Animal protocols were approved by the Institutional Animal Care and Use Committee at Virginia Polytechnic Institute and State University. Female Balb/c mice (6–7 weeks, 16–20 g, 8 per group) were randomized into vaccine and control groups. The immunization schedules and administration doses are shown in Table I. Vaccine groups (Groups 1–5) were immunized subcutaneously (s.c.) with 100 μL of a saline suspension of Nic-BSA conjugates, or Nic-BSA-liposome conjugates or Nic-BSA-nanohorn-liposome conjugates mixed with or without Alum adjuvant (3 mg, Imject, Pierce Biotechnology Inc., Rockford, IL). Control groups (Groups 6 and 7) received liposomes or nanohorn-supported-liposomes formulated with Alum (3 mg) in 100 μL saline. All mice were immunized with three injections, given on day 0 with booster immunizations on days 14 and 28. Antibody titers were monitored following vaccine administration using blood samples (~200 μL) taken on days 0, 13, 27, 33, 40 from the retroorbital plexus of mice under isofluorane anesthesia. The blood samples were kept at 37 °C for 30 min and then centrifuged at 4 °C at 2000×*g* for 30 min, with the supernatant centrifuged a second time. Aliquots of sera were stored at −80 °C prior to analysis.

Author Manuscript Author Manuscript Author Manuscript Author Manuscript

Measurement of Specific Anti-Nicotine IgG Antibodies Using ELISA—Mice sera were analyzed according to the ELISA procedure described by de Villiers et al. with appropriate modification.[38] Briefly, the nicotine hapten was conjugated to keyhole limpet hemocyanin (KLH) according to the same method used for the preparation of Nic-BSA conjugate. MICROLON® 96 well plates (Greiner Bio-One, Longwood, FL) were coated with Nic-KLH conjugate (10 μg/mL in carbonate buffer, 0.05 M, pH 9.6, 100 μL/well) and incubated at 25 °C for 5 h. The plates were washed with PBS-Tween (0.1%) for 4 times and distilled water for 2 times, followed by blocking with 300 μL Pierce® protein-free T20 blocking buffer for 12 h. Sera from immunized mice were serially diluted at different dilution (1:25, 1:125, 1:625, 1:3125, 1:15625, and 1:78125) in PBS, and 100 μL of each dilution was added to the plate which was subsequently incubated at 25 °C for 2 h. The plates were washed again, and incubated with 100 μL Anti-Mouse IgG HRP (1:10000) from Alpha Diagnostic Intl (San Antonio, TX) for 1 h. After washing as before, plates were incubated with tetramethylbenzidine (TMB) peroxidase (100 μL/well) for 10 min in the dark. Sulphuric acid was added (0.5%, 100 μL/well) and absorbance was measured at 450 nm, using a Microplate Reader (Synergy HTS Multi-Mode, BioTek Instruments, Inc., Winooski, VT). The ELISA titer was defined as the dilution of the serum which gives a half-maximal optical density signal (OD 50%) in the ELISA.

Determination of Anti-Nicotine Specific IgG Subclasses—For the IgG subtype determination, duplicate ELISA were done for the four antibody isotypes in serum from mice of each group. Horseradish peroxidase conjugated sheep anti-mouse IgG1, IgG2a, IgG2b and IgG3 (Alpha Diagnostic Intl.) were used as the secondary antibodies.

Th1/Th2 Index Calculation—To determine whether the addition of nanohorn, liposomes and Alum adjuvant in the immunization protocol induced a Th1 (IgG2a and IgG3) or Th2 (IgG1) polarization, Th1:Th2 index was calculated as ([IgG2a+IgG3]/2)/(IgG1) for each immunization groups. According to such calculation, an index value <1 stands for a Th2 polarization; an index value >1 stands for a Th1 polarization.[39]

Antibody Affinity for Nicotine Evaluation by Equilibrium Dialysis—In order to assess antibody affinity (K_d) and maximum nicotine binding capacity (B_{max}), sera from immunized mice treated with NsL-based anti-nicotine vaccine in the presence and absence of Alum on day 40 were diluted with control sera (Balb/C mouse serum, Innovative Research Inc., Novi, MI), due to small sample sizes. These were then dialyzed against six different concentrations of nicotine using a 96-well Equil DIALYZER (MWCO 10 kD, the Nest Group, Inc. Southborough, MA). Unlabeled ((-)-nicotine hydrogen tartrate salt, Sigma-Aldrich, St. Louis, MO) and tritiated nicotine, (L-(-)-[N-methyl-3H]-nicotine, PerkinElmer, Boston, MA) were diluted in control sera to total nicotine concentrations ranging from 1 ng/mL to 1024 ng/mL (expressed as free base). The plate was placed vertically on a shaker and incubated for 72 h at room temperature, until equilibrium had been reached. Samples from both sides of the dialysis membrane were collected and counted using a 1450 MicroBeta TriLux Liquid scintillation counter (EG&G Wallac) with MicroBeta workstation software (version 2.7). Disintegrations per minute (DPM) were transformed to total nicotine concentrations based on the radioactivity of the original solutions. Bound versus free

Author Manuscript Author Manuscript Author Manuscript Author Manuscript

nicotine was plotted to create a saturation binding curve from which K_d, the concentration resulting in half of the binding sites being occupied, and B_{max} (GraphPad Prism 5, GraphPad Software, Inc.) were determined. Values for B_{max} were adjusted for the serum dilution.

Mouse Toxicology Studies

Animals and Animal Husbandry—This study was conducted in accordance with the U.S. Food and Drug Administration *Good Laboratory Practice Regulations for Nonclinical Laboratory Studies*,[40, 41] with the *Guide for the Care and Use of Laboratory Animals*,[42] and under a protocol approved by the Institutional Animal Care and Use Committee at Virginia Polytechnic Institute and State University.

The experimental animals were female Balb/cByJ mice (The Jackson Laboratory, Inc., Bar Harbor, ME, USA), 5 weeks old upon arrival. The Balb/c mouse was chosen to conform to the requirements by the National Toxicology Program (NTP).[43, 44] Animals were individually identified by ear notching during a 7-day quarantine. The study began after the quarantine when the mice were 6 weeks old. Mice were housed individually in solid-bottom, polycarbonate cages with stainless steel lids (Laboratory Products, Rochelle Park, NJ) and Certified Sani-Chip® hardwood cage litter (P. J. Murphy, Montville, NJ). Feed (Purina Certified Rodent Chow (#5002), PMI, St. Louis, MO) and tap water (Blacksburg, VA) were provided *ad libitum* throughout the study. The light cycle (12 h light, 12 h dark) and temperature and relative humidity in the animal rooms were controlled and monitored (Siebe/Barber-Coleman Network 8000® System with SIGNAL® Software [Version 4.1], Siebe Environmental Controls (SEC)/Barber-Colman Company, Loves Park, IL) throughout the study. Temperature and relative humidity were within their respective target ranges (69–75 °F and 35–65%).

Evaluation of Body Weight, Feed and Water Consumption, and Clinical Signs—After the 7-day quarantine, the animals were randomly divided into seven groups containing eight animals per group. During the treatment period of seven weeks (see section on Immunization procedures, 2.7.1), body weight, feed consumption, and water consumption were measured by the method of McNair and Bryson[45] and recorded twice per week. In the studies, clinical signs of toxicity included body condition, lethargy, abnormal posture, and ruffled fur.

Evaluation of Organ/Body Weight Ratios—On day 45, after 7 weeks of observation described above, all animals were weighed and then euthanized under CO_2. The hearts, lungs, livers, spleens and kidneys were excised and weighed accurately. Organ/body weight ratios were calculated as organ weight/body weight × 100 (%).[46]

Histopathological Evaluation—Histopathological analysis of hearts, lungs, livers, spleens, kidneys and skin tissues from the vaccine sites of each experiment group was performed by the method of Iranloye and Bolarinwal.[47] Briefly, organs (hearts, lungs, livers, spleens, kidneys and skins) were fixed in a neutral 10% buffered formalin. Then tissue blocks were embedded in paraffin and routine sections stained as described by Lillie with hematoxylin and eosin.[48] After hematoxylin-eosin (HE) staining, sections were examined by

Author Manuscript Author Manuscript Author Manuscript Author Manuscript

light microscopy on a Nikon Eclipse E600 scope and images captured using a Nikon DS-Fi1 camera run by NIS Elements software (Nikon, Melville, NY).

Statistical Analysis

Statistical analysis was performed using the Student's *t*-test for the difference between the experimental groups and the control group. Bonferroni correction was used where multiple comparisons were made. Differences between means were considered significant at $P < 0.05$, very significant at $P < 0.01$ and highly significant at $P < 0.001$.

RESULTS AND DISCUSSION

Conjugating Antigen to Nanohorn-Supported-Liposomes

In this present study, nicotine derivative, O-succinyl-3′-hydroxmethyl-(±) nicotine[26] was used as the target hapten. Antibodies induced by this hapten (coupled to virus-like particles derived from the coat protein of the bacteriophage Qb) have been shown to have a high affinity for nicotine (K_d = 35 nM) and no cross-reactivity with acetylcholine, the major nicotine metabolites cotinine and nicotine-*N*-oxide, and a variety of other neurotransmitters or drugs. Bovine serum albumin (BSA) acted as a model carrier protein to conjugate with the hapten in this study. BSA (67 kD) is a commonly used model carrier protein in vaccine development. For example, the anti-cancer vaccine, in which BSA was conjugated with 3′-fluoro-TF antigen-MUC1, was able to generate high titers of antibodies that could specifically bind to a tumor-associated glycopeptide antigen analog.[49]

Covalent attachment of carboxylic acid hapten to the carrier protein (BSA) via available surface amino groups on BSA (26 surface lysines) was confirmed by reacting the prepared conjugates with TNBS reagent. The number of amino groups present in the carrier protein before and after conjugation was quantified with a UV/Vis spectrophotometer (Shimadzu 1601) set at 335 nm. The gradual decrease of the available surface lysines on the protein after reaction with different molar ratios of hapten confirmed the increase in conjugation density (number of hapten molecules per protein molecule) with the increasing hapten-protein molar ratio.

Conjugation of protein to the liposome surface was based on a chemical reaction between the maleimide of the PEGylated lipid with a derivatized sulfhydryl group at the primary amines of a protein by adding Traut's reagent, as previously described for conjugation of lactoferrin to the liposome surface.[50] The thiolation level was measured using 5,5′-dithiobis(2-nitrobenzoic acid) (Ellman's reagent) as described by Benzinger et al.[51] By optimizing the molar ratio of BSA:Nic:Traut's reagent:DSPE-Mal-PEG2000, higher association efficiency of Nic-BSA to NsL can be obtained (Table II). Conjugates with 15 Nic haptens per BSA were produced by using a 50-fold excess of Nic-hapten. A 200-fold excess of 2-iminothiolane resulted in 5 thiol groups per Nic-BSA conjugate molecule. Moreover, a ratio of 1:4 or 1:8 of Nic-BSA:DSPE-Mal-PEG2000 was used for conjugation, and a strong antigen-NsL association efficiency of 50.4% or 65.8% and loading efficiency of 21.7% or 25.3% were achieved, respectively.

Author Manuscript Author Manuscript Author Manuscript Author Manuscript

Physicochemical Properties of NsL NPs

Particle Size, Zeta Potential Analysis—The particle sizes and zeta potentials of nanohorns, liposomes, NsL and Nic-BSA-NsL are presented in Table III. The results show that the mean diameter of nanohorns, liposomes, NsL and Nic-BSA-NsL was 107.8 ± 3.3, 152.0 ± 6.0, 164.9 ± 2.5 and 175.3 ± 3.2 nm, respectively, suggesting there was no significant difference in size after the encapsulation of a nanohorn in a cationic liposome and the conjugation of antigens. In addition, the DLS analysis results of nanoparticle size agree well with the size obtained by TEM (Fig. 1). The zeta potentials of liposomes were around 40 mV regardless of the presence of nanohorn, suggesting that negatively charged nanohorns embedded into the cationic liposomes did not significantly change the zeta potential of the liposome nanoparticles. It has been suggested that full electrostatic stabilization requires a zeta potential >30 mV (ideally >60 mV), potentials between 5 mV and 15 mV result in limited flocculation, and potentials between −5mV and +3mV yield maximum flocculation.[5253] Therefore, the zeta potentials obtained in the present study were within the range of full electrostatic stabilization, and values near 40 mV indicate the presence of strong forces of repulsion among the nanoparticles and little tendency for aggregation. Furthermore, charged nanoparticles adsorbed to the liposome can provide additional steric stabilization of liposomes.[37] Thus the nanohorn-supported liposomes prepared in this study should, therefore, remain stable for a relatively long period of time.

TEM Analysis—Figure 1 shows TEM images of nanohorns, empty liposomes, and nanohorn supported liposome nanoparticles. Evidently, carbon nanohorns are nearly spherical particles, approximately 100 nm in diameter, with a so-called ‘dahlia flower’ structure[24] (Fig. 1(A)). The empty DOTAP liposomes and the nanohorn supported liposome nanoparticles (NsL) have nearly spherical shapes with sizes of 100–300 nm (Figs. 1(B), (C)). The size of the nanoparticles observed by TEM was consistent with the results of dynamic light scattering (Table III). As shown in Figure 1(C), a nanohorn supported liposome is a combination of the particles shown in Figures 1(A) and (B).

Liposomes with diameters of less than 500 nm were shown to efficiently enhance the immunogenic performance of liposome vaccines over large liposomes (>500 nm).[54] This is expected because the optimal particle diameter for uptake by APCs is below 500 nm. Particles of small size are also essential if non-liposome vectors are to induce a high immune response. For example poly(D,L-lactic-co-glycolic acid) (PLGA) particles of 300 nm loaded with DNA induced much higher antibody titers than particles with a diameter of 1 μm.[55] Moreover, for the present study, nicotine haptens were designed to bind to the surface of liposomes, and thus small nanohorn supported liposome nanoparticles will not only fit the size requirement of particles preferred for APC uptake but also provide the higher surface/volume ratio that increases capacity for hapten loading.

Stability of Nanohorn Supported Liposome Nanoparticles—The efficiency of liposomes as a delivery vehicle is usually compromised after administration into human body by liposomal instability during storage or circulation.[56] The instability can be caused by oxidation, degradation or fusion of liposomes with each other.[57, 58] In vaccine development, the desirable size of liposomes should be less than 300 nm due to uptake

Author Manuscript Author Manuscript Author Manuscript Author Manuscript

preference of the major antigen presenting cells (especially dendritic cells). However, the fusion of liposomes tends to result in particles with larger size. Many strategies can overcome this problem, and among them, including PEGylation of the liposomes. Despite the stabilizing effect on liposomes, PEGylation may lead to reduced uptake of liposomes by target cells due to reduced interaction between liposomes and cells.[5659] In this study, negatively charge nanohorns were the scaffold introduced into positively charged liposomes. Figure 2 shows that during liposome preparation, nanohorn supported liposomes exhibited better uniformity and smaller size than blank liposomes. Aggregates in Figure 2(A) indicate that even during preparation, liposome tended to fuse with each other to form larger particles. However, liposomes supported by nanohorns displayed smaller and more uniform morphology (Fig. 2(B)). Significant fusion occurred with liposomes alone after storage for 5 days at 4 °C, as shown by the clusters in Figure 2(C). In addition, the presence of smaller particles in Figure 2(C) suggests that some degradation also occurred. Although increased size was detected in nanohorn supported liposomes, many still maintained their original size (Fig. 2(D)). The comparison between liposome images with and without nanohorns suggests that nanohorns exerted a stabilizing effect on liposomes during both preparation and storage.

Immunogenicity Study

Time Course for Serum IgG Antibody Responses to Nic-BSA, Nic-BSA-LIP and Nic-BSA-NsL Immunization by Subcutaneous Injection With or Without Alum

—The development of anti-nicotine immune response was determined by analyzing serum samples collected during animal study using ELISA. ELISA plates were coated with Nic-KLH conjugates. The results demonstrated that all subcutaneously-administered vaccines, each containing 50 μg Nic-BSA, resulted in gradual increase of serum anti-nicotine IgG antibody titers (Fig. 3). This occurred both in the presence and absence of Alum. Maximum titers were obtained two weeks after the second booster of a vaccine. Nicotine-specific IgG antibody (NicAb) titers in the presence of Alum were higher than those in the absence of Alum in groups given Nic-BSA-LIP and Nic-BSA-NsL (Fig. 3). No NicAb were detected in sera collected on day 0, showing that Nic vaccine treatment was necessary for the production of antibodies. After the primary immunization and two additional boosters, the titer of NicAb elicited in response to Nic-BSA-NsL with Alum was significantly greater than titers in other groups whether or not the vaccines were given with or without Alum. In addition, even in the absence of Alum, a significant level of nicotine-specific antibodies could be observed in the Nic-BSA-NsL group.

In this study an NsL-based anti-nicotine vaccine delivery system was developed. When administered subcutaneously, the vaccine elicited a strong immune response, inducing 5 and 7 fold increases in total IgG titers compared to the anti-nicotine vaccine (Nic-BSA) formulated with or without liposomes, respectively. It is worth noting that the total antibody titer for Nic-BSA-NsL, even with the absence of Alum, is similar to the titer of the nicotine vaccine by Selecta Biosciences, SEL-068 (5×10^5 for Nic-BSA-NsL, 1×10^6 for SEL-068), which, based on the limited available information, has haptens conjugated to the surface of the nanoparticles and a universal antigen peptide encapsulated inside the nanoparticles.[60] It has also been reported that the anti-nicotine vaccine, which is based on virus-like particles (VLPs) of the RNA phage Qb to which nicotine haptens are covalently coupled via

Author Manuscript Author Manuscript Author Manuscript Author Manuscript

succinimate linkers (NicQb), induced potent and long-lived antibody responses in mice[61] as well as humans.[62–64] Compared with the hapten delivered by the virus-like particles, NicQb by Cytos AG,[61, 65] this nano-vaccine was larger in size (~100 nm compared to 25 nm) and contained lipids that induced a stronger immune response.

Detection of Subclass Distribution of Nicotine-Specific Antibodies After Vaccination—Human IgG consists of four subclasses contributing in different ways to humoral immunity against pathogens. Mice, similarly to humans, have four different classes of IgGs, namely IgG1, IgG2a, IgG2b and IgG3, which functionally correspond to the human IgG1, IgG2, IgG4 and IgG3, respectively. Despite some species differences in the IgG subclasses, the overall structure of the humoral IgG pattern in mice and humans are quite similar. In general, mouse IgG1 (as well as IgG4 in humans) is associated with a Th2 profile and the other subclasses are mainly associated with a Th1 profile.[66] In this study, the pattern of IgG subclasses induced by the different anti-nicotine vaccines was evaluated by using secondary goat anti-mouse antibodies specific for each IgG subclass. Sera from animals immunized with Nic-BSA + Alum showed low titers (3182, 16 and 9, respectively) of both Th2- associated IgG1 subclasses and Th1-associated IgG2a and IgG3 subclasses (Fig. 4). Liposome-based anti-nicotine vaccines (Nic-BSA-LIP) in the presence and absence of Alum adjuvant did not significantly enhance IgG1 and IgG3 titers, but induced a 100-fold enhancement in anti-Nicotine IgG2a titers (1859 and 1492, respectively) compared to Nic-BSA + Alum (Fig. 4). In contrast, NsL-based anti-nicotine vaccines (Nic-BSA-NsL) in the presence and absence of Alum adjuvant induced significantly higher titers of all four IgG subclasses (Fig. 4), with the highest titers observed for Th2-associated subclasses (IgG1 ⩾ Ig2a > Ig2b > Ig3). Evaluation of IgG subclasses demonstrated that NsL-based anti- nicotine vaccines are capable of inducing stronger humoral immune responses, indicated by the induction of significant antigen specific IgG1 and IgG2a titers.

Th1:Th2 Index Calculation—To assess whether NsL, LIP and Alum adjuvant formulation elicited a specific IgG subclass profile or induced an increase in all subclasses, a Th1:Th2 index was calculated for each vaccine (Table IV). Such index takes into consideration of both Th1-associated IgG2a and IgG3 subclasses and Th2-associated IgG1 subclass. The Th1:Th2 index shows that, in sera of animals immunized with Nic-BSA + Alum, the antibody response to nicotine was Th2 polarized and Th1:Th2 index was 0.004. However, both Th2-related IgG1 and Th1-related IgG2a and IgG3 antibody responses were all significantly elevated in the mice vaccinated with the Nic-BSA using NsL or LIP-based vaccine delivery ($P < 0.001$) (Fig. 4 and Table IV). In addition, Th1/Th2 balance was improved after vaccination using NsL or LIP-based vaccine delivery even in the absence of Alum adjuvant (Th1:Th2 index 0.085 and 0.160, respectively) (Table IV).

Vaccine-induced immune responses can be generally divided into two different biased effects: Th1 versus Th2 types. Many factors can contribute to the type of specific immune response of a vaccine, including the type and relative amounts of antigens and adjuvants. Aluminum salts as adjuvant generally are well known to induce a Th2-type immune response.[67, 68] On the contrary, liposomes developed as potential adjuvants generally elicit a Th1-type immune response.[69] In addition, Balb/c and C57BL/6 are widely used mouse

Author Manuscript Author Manuscript Author Manuscript Author Manuscript

strains, showing polarized Th cell responses. Balb/c mice typically develop Th2-skewed immune responses, whereas C57BL/6 mice are prone to Th1-dominated immunity.[70] Our results demonstrated that NsL or LIP modulated immune responses from a predominantly Th2 type response to a mixed Th1/Th2 response. Results also demonstrated that NsL-based anti-nicotine vaccine delivered by subcutaneous administration to Balb/c mice can not only significantly enhance both Th1 and Th2 immune responses but also improve Th1/Th2 balance. However, the immunological mechanism of this effect is not clear and requires further investigation.

Antibody Affinity to Nicotine—Individual serum sample was diluted with control mice serum and dialyzed against 5 different nicotine concentrations. From this saturation binding experiment, the affinity (K_d), and maximum number of binding sites (B_{max}) were determined. The antibody concentration was calculated from the B_{max}, assuming two binding sites per antibody molecule and a molecular weight of the antibody of 150 kD. Both values were obtained by calculating back to undiluted sera. The equilibrium dialysis method does not require any washing steps that might wash away low affinity antibodies, so total binding is measured. At the time the last blood sample was collected, the K_d for nicotine was $5.84\times10^2 \pm 1.86\times10^2$ nM and the B_{max} was $2.85\times10^3 \pm 1.26\times10^3$ nM, corresponding to $2.14\times10^2 \pm 0.95\times10^2$ μg/mL of nicotine-specific IgG in the group of mice immunized with NsL-based anti-nicotine vaccine without Alum. For the group of mice given NsL-based anti-nicotine vaccine with Alum, K_d and B_{max} were $1.27\times10^3 \pm 0.58\times10^3$ and $4.14\times10^3 \pm 1.04\times10^3$ nM, respectively, which were equivalent to $3.11\times10^2 \pm 0.61\times10^2$ μg/mL of nicotine-specific IgG. Our results demonstrated that NsL-based anti-nicotine vaccines prepared in the absence of Alum generated an anti-nicotine antibody with high affinity and a high concentration in the serum of vaccinated mice.

Preclinical Animal Toxicity Studies

Body Weights, Feed, and Water Consumption—Mice continued to grow during their 7-week treatment with anti-nicotine vaccines. Behaviors such as feeding, drinking and activity were normal in all seven groups and there were no overt signs of toxicity. Mean body weights, weight gains, feed consumption and water consumption were all equivalent ($P > 0.05$) (Table V). Although nicotine administration can induce weight loss and change eating behavior in both humans and rodents,[71–73] there was no significant difference between the mice in the vaccinated groups and the mice in the control groups. Our vaccines were formulated with low doses of nicotine hapten-BSA conjugates, which may have contributed to this benefit.

Gross Pathology—Toxicities may also be indicated by changes in tissue or organ weight, size, color, and gross appearance. Table VI shows body weight and organ/body weight ratios (%) of the liver, kidney, spleen, lung and heart of mice in the five vaccinated groups and two control groups. No significant differences were measured between the treated and the control groups ($P > 0.05$).

Histopathological Assessment—Histopathological review indicated that there were no significant lesions in the heart, lung, liver, spleen and kidney of mice in the two control

Author Manuscript Author Manuscript Author Manuscript Author Manuscript

groups and the five vaccinated groups whether or not Alum was included in the vaccines (examples provided in Figs. 5(A)–(E)). However, occasional background lesions were noted, especially in mice vaccinated with Alum. For example, all of these mice had subcutaneous necrosis with associated granulomatous inflammation (Fig. 5(F)), some of which included focal epicardial calcification.[74] A pulmonary embolus was also seen in the group of mice vaccinated with LIP with Alum. This finding of subcutaneous lesions is in agreement with the report of Goto et al. suggesting that Alum injection was responsible for the induction of granulomas at the injection sites of guinea pigs.[75] Aluminum adjuvants have been commonly used both in veterinary and human vaccines for many years,[76, 77] but they occasionally produce subcutaneous nodules,[7879] granulomatous inflammation[69, 80–82] and sterile abscesses[72] as local side reactions. Although seen in Alum-treated mice in this study, NsL-based anti-nicotine vaccines without Alum did not induce any histopathologic lesions at injection sites.

CONCLUSIONS

A novel anti-nicotine vaccine, based on NsL NPs, has been successfully developed. The carbon nanohorns are negatively charged (anionic) and act as a scaffold for the assembly of cationic liposomes. NsL NPs were stable after an extended period of storage. The nano-vaccine induced strong, anti-nicotine antibody responses in mice when administrated subcutaneously, leading to production of high titer and high affinity anti-nicotine antibodies for treatment of nicotine dependence. The total antibody titer for NsL-based anti-nicotine vaccine, even without the presence of Alum, reached ~5×10^5. The K_d for nicotine was $5.84 \times 10^2 \pm 1.86\times10^2$ nM and B_{max} was $2.85\times10^3 \pm 1.26 \times10^3$ nM corresponding to $2.14\times10^2 \pm 0.95 \times 10^2$ μg/mL of nicotine-specific IgG for this nano-vaccine without Alum. In addition, evaluation of IgG subclasses demonstrated that NsL-based anti-nicotine vaccine was capable of inducing a more balanced Th1 and Th2 response. Furthermore, the safety evaluation of NsL NPs in mice revealed no apparent toxicity.

Acknowledgments

This research was supported by National Institute on Drug Abuse (R21 DA030083, PI: C. Zhang). We are grateful to Dr. B. Jortner for his assistance in histopathological evaluations.

References

1. Esson, L., Leeder, SR. The millennium development goals and tobacco control: An opportunity for global partnership. World Health Organization (WHO); Geneva: 2004.
2. World Health Organization. Why is tobacco a public health priority? A tobacco free initiative. 2005
3. Aubin HJ, Karila L, Reynaud M. Pharmacotherapy for smoking cessation: Present and future. Curr Pharm Des. 2011; 17:1343. [PubMed: 21524268]
4. Hays JT, Ebbert JO. Adverse effects and tolerability of medications for the treatment of tobacco use and dependence. Drugs. 2010; 24:2357.
5. The Health Consequences of Smoking, Centers for Disease Control and Prevention USA. Surgeon's General Report. 2004
6. Moreno AY, Janda K. Immunopharmacotherapy: Vaccination strategies as a treatment for drug abuse and dependence. Pharmacol Biochem Behav. 2009; 92:199. [PubMed: 19350728]

Author Manuscript Author Manuscript Author Manuscript Author Manuscript

7. Cornuz J, Zwahlen S, Jungi WF, Osterwalder J, Klingler K, van Melle G, Bangala Y, Guessous I, Müller P, Willers J, Maurer P, Bachmann MF, Cerny T. A vaccine against nicotine for smoking cessation: A randomized controlled trial. PLoS One. 2008; 3:e2547. [PubMed: 18575629]
8. Cerny EH, Cerny T. Vaccines against nicotine. Hum Vaccin. 2009; 5:200. [PubMed: 19276649]
9. News release, Nabi Biopharmaceuticals. Nov 7. 2011 http://phx.corporate-ir.net/phoenix.zhtml?c=100445&p=irol-news
10. Hicks MJ, Rosenberg JB, De BP, Pagovich OE, Young CN, Qiu J, Kaminsky SM, Hackett NR, Worgall S, Janda KD, Davisson RL, Crysal RG. AAV-directed persistent expression of a gene encoding anti-nicotine antibody for smoking cessation. Sci Transl Med. 2012; 4:140ra87.
11. Kwon YJ, James E, Shastri N, Fréchet JM. *In vivo* targeting of dendritic cells for activation of cellular immunity using vaccine carriers based on pH-responsive microparticles. Proc Natl Acad Sci USA. 2005; 102:18264. [PubMed: 16344458]
12. Akagi T, Wang X, Uto T, Baba M, Akashi M. Protein direct delivery to dendritic cells using nanoparticles based on amphiphilic poly(amino acid) derivatives. Biomaterials. 2007; 28:3427. [PubMed: 17482261]
13. Coester C, Nayyar P, Samuel J. *In vitro* uptake of gelatin nanoparticles by murine dendritic cells and their intracellular localisation. Eur J Pharm Biopharm. 2006; 62:306. [PubMed: 16316749]
14. Yeboah KG, D'souza MJ. Evaluation of albumin microspheres as oral delivery system for Mycobacterium tuberculosis vaccines. J Microencapsul. 2009; 26:166. [PubMed: 18608796]
15. Chikh G, Schutze-Redelmeier MP. Liposomal delivery of CTL epitopes to dendritic cells. Biosci Rep. 2002; 22:339. [PubMed: 12428909]
16. Copland MJ, Baird MA, Rades T, McKenzie JL, Becker B, Reck F, Tyler PC, Davies NM. Liposomal delivery of antigen to human dendritic cells. Vaccine. 2003; 21:883. [PubMed: 12547598]
17. Shahum E, Thérien HM. Effect of liposomal antigens on the priming and activation of the immune system by dendritic cells. Int Immunopharmacol. 2002; 2:591. [PubMed: 11962737]
18. Moribe K, Maruyama K. Pharmaceutical design of the liposomal antimicrobial agents for infectious disease. Curr Pharm Des. 2002; 8:441. [PubMed: 12069381]
19. Sprott GD, Dicaire CJ, Gurnani K, Deschatelets LA, Krishnan L. Liposome adjuvants prepared from the total polar lipids of Haloferax volcanii, Planococcus spp. and Bacillus firmus differ in ability to elicit and sustain immune responses. Vaccine. 2002; 22:2154.
20. Alving CR, Koulchin V, Glenn GM, Rao M. Liposomes as carriers of peptide antigens: Induction of antibodies and cytotoxic T lymphocytes to conjugated and unconjugated peptides. Immunol Rev. 1995; 145:5. [PubMed: 7590830]
21. Laughlin RG. Equilibrium vesicles: Fact or fiction? Colloids Surf A. 1997; 128:27.
22. Miyawaki J, Yudasaka M, Azami T, Kubo Y, Iijima S. Toxicity of single-walled carbon nanohorns. ACS Nano. 2008; 2:213. [PubMed: 19206621]
23. Lynch RM, Voy BH, Glass DF, Mahurin SM, Zhao B, Hu H, Saxton AM, Donnell RL, Cheng MD. Assessing the pulmonary toxicity of single-walled carbon nanohorns. Nanotoxicology. 2007; 1:157.
24. Iijima S, Yudasaka M, Yamada R, Bandow S, Suenaga K, Kokai F, Takahashi K. Nano-aggregates of single-walled graphitic carbon nanohorns. Chem Phys Lett. 1999; 309:165.
25. Huang W, Zhang J, Dorn HC, Geohegan D, Zhang C. Assembly of single-walled carbon nanohorn supported liposome particles. Bioconjug Chem. 2011; 22:1012. [PubMed: 21528932]
26. Maurer P, Jennings GT, Willers J, Rohner F, Lindman Y, Roubicek K, Renner WA, Müller P, Bachmann MF. A therapeutic vaccine for nicotine dependence: Preclinical efficacy, and phase I safety and immunogenicity. Eur J Immunol. 2005; 35:2031. [PubMed: 15971275]
27. Kasuya D, Yudasaka M, Takahashi K, Kokai F, Iijima S. Selective production of single-wall carbon nanohorn aggregates and their formation mechanism. J Phys Chem B. 2002; 106:4947.
28. Zhang J, Ge J, Shultz MD, Chung E, Singh G, Shu C, Fatouros PP, Henderson SC, Corwin FD, Geohegan DB, Puretzky AA, Rouleau CM, More K, Rylander C, Rylander MN, Gibson HW, Dorn HC. *In vitro* and *in vivo* studies of single-walled carbon nanohorns with encapsulated metallofullerenes and exohedrally functionalized quantum dots. Nano Lett. 2010; 10:2843. [PubMed: 20698597]

Author Manuscript Author Manuscript Author Manuscript Author Manuscript

29. Shu C, Zhang J, Ge J, Sim JH, Burke BG, Williams KA, Rylander NM, Campbell T, Puretzky A, Rouleau C, Geohean DB, More K, Esker AR, Gibson HW, Dorn HC. A facile high-speed vibration milling method to water-disperse single-walled carbon nanohorns. Chem Mater. 2010; 22:347.
30. Hu Y, Zheng H, Huang W, Zhang CM. A novel and efficient nicotine vaccine using nano- lipoplex as a delivery vehicle. Hum Vaccin Immunother. 2014; 10:1. [PubMed: 24832715]
31. Habeeb AFSA. Determination of free amino groups in proteins by trinitrobenzene-sulfonic acid. Anal Biochem. 1966; 14:328. [PubMed: 4161471]
32. Jue R, Lambert JM, Pierce LR, Traut RR. Addition of sulfhydryl groups to Escherichia coli ribosomes by protein modification with 2-iminothiolane (methyl 4-mercaptobutyrimidate). Biochemistry. 1978; 17:5399. [PubMed: 365229]
33. Ansell SM, Tardi PG, Buchkowsky SS. 3-(2-pyridyldithio)propionic acid hydrazide as a cross-linker in the formation of liposome-antibody conjugates. Bioconjug Chem. 1996; 7:490. [PubMed: 8853463]
34. Ansell SM, Harasym TO, Tardi PG, Buchkowsky SS, Bally MB, Cullis PR. Antibody conjugation methods for active targeting of liposomes. Methods Mol Med. 2000; 25:51. [PubMed: 21318840]
35. Kaszuba M, Corbett J, Watson FM, Jones A. High-concentration zeta potential measurements using light-scattering techniques. Philos Transact A Math Phys Eng Sci. 2010; 368:4439.
36. Kodama T, Tomita N, Horie S, Sax N, Iwasaki H, Suzuki R, Maruyama K, Mori S, Manabu F. Morphological study of acoustic liposomes using transmission electron microscopy. J Electron Microsc (Tokyo). 2010; 259:187.
37. Zhang L, Granick S. How to stabilize phospholipid liposomes (using nanoparticles). Nano Lett. 2006; 6:694. [PubMed: 16608266]
38. de Villiers SH, Lindblom N, Kalayanov G, Gordon S, Baraznenok I, Malmerfelt A, Marcus MM, Johansson AM, Svensson TH. Nicotine hapten structure, antibody selectivity and effect relationships: Results from a nicotine vaccine screening procedure. Vaccine. 2010; 28:2161. [PubMed: 20060511]
39. Visciano ML, Tagliamonte M, Tornesello ML, Buonaguro FM, Buonaguro L. Effects of adjuvants on IgG subclasses elicited by virus-like particles. J Transl Med. 2012; 10:4. [PubMed: 22221900]
40. U.S. FDA. U.S. Food and Drug Administration. Good Laboratory Practice Regulations for Nonclinical Laboratory Studies. CFR. Apr 1.1988 :229–243.
41. U.S. FDA. U.S. Food and Drug Administration. Good Laboratory Practice Regulations for Nonclinical Laboratory Studies. CFR. Mar 21.1994 :56FR12300.
42. NRC Guide for the Care and Use of Laboratory Animals. National Academy Press; Washington, DC: 1996.
43. Collins TF, Sprando RL, Shackelford ME, Hansen DK, Welsh JJ. Food and Drug Administration proposed testing guidelines for developmental toxicity studies. Regul Toxicol Pharmacol. 1999; 30:39. [PubMed: 10464045]
44. WHO guidelines on nonclinical evaluation of vaccines. Nov 17–21. 2003 p. 9-12.WHO Technical Report Series
45. McNair E, Bryson R. Effects of nicotine on weight change and food consumption in rats. Pharmacol Biochem Behav. 1983; 18:341.
46. Pecora LJ, Highman B. Organ weights and histology of chronically thiamine-deficient rats and their pair-fed controls. J Nutr. 1953; 51:219. [PubMed: 13097238]
47. Iranloye BO, Bolarinwa AF. Effect of nicotine administration on weight and histology of some vital visceral organs in female albino rats. Niger J Physiol Sci. 2009; 24:7. [PubMed: 19826458]
48. Lillie, RD. Histopathologic Technic. The Blakiston Co; Philadelphia, PA: 1948.
49. Hoffmann-Roder A, Johannes M. Synthesis of a MUC1-glycopeptide-BSA conjugate vaccine bearing the 3′-deoxy-3′-fluoro-Thomsen-Friedenreich antigen. Chem Commun (Camb). 2011; 47:9903. [PubMed: 21818465]
50. Huang FY, Chen WJ, Lee WY, Lo ST, Lee TW, Lo JM. *In vitro* and *in vivo* evaluation of lactoferrin-conjugated liposomes as a novel carrier to improve the brain delivery. Int J Mol Sci. 2013; 14:2862. [PubMed: 23434652]

Author Manuscript Author Manuscript Author Manuscript Author Manuscript

51. Benzinger P, Martiniy-Baron G, Reusch P, Siemeister G, Kley JT, Marmé D, Unger C, Massing U. Targeting of endothelial KDR receptors with 3G2 immunoliposomes *in vitro*. Biochim Biophys Acta. 2000; 1466:71. [PubMed: 10825432]
52. Schwarz C, Mehnert W, Lucks JS, Muller RH. Solid lipid nanoparticles (SLN) for controlled drug delivery. I. Production, characterization and sterilization. J Control Release. 1994; 30:83.
53. Alves C, de Melo N, Fraceto L, de Araújo D, Napimoga M. Effects of 15d-PGJ2-loaded poly(D,L-lactide-co-glycolide) nanocapsules on inflammation. Br J Pharmacol. 2011; 162:623. [PubMed: 20883476]
54. Carstens MG, Camps MG, Henriksen-Lacey M, Franken K, Ottenhoff TH, Perrie Y, Bouwstra JA, Ossendorp F, Jiskoot W. Effect of vesicle size on tissue localization and immunogenicity of liposomal DNA vaccines. Vaccine. 2011; 29:4761. [PubMed: 21565240]
55. Singh M, Briones M, Ott G, O'Hagan D. Cationic microparticles: A potent delivery system for DNA vaccines. Proc Natl Acad Sci USA. 2000; 97:811. [PubMed: 10639162]
56. Pornpattananangkul D, Olson S, Aryal S, Sartor M, Huang CM, Vecchio K, Zhang L. Stimuli-responsive liposome fusion mediated by gold nanoparticles. ACS Nano. 2010; 4:1935. [PubMed: 20235571]
57. Pietzyk B, Henschke K. Degradation of phosphatidylcholine in liposomes containing carboplatin in dependence on composition and storage conditions. Int J Pharm. 2000; 196:215. [PubMed: 10699721]
58. Stark B, Pabst G, Prassl R. Long-term stability of sterically stabilized liposomes by freezing and freeze-drying: Effects of cryoprotectants on structure. Eur J Pharm Sci. 2010; 41:546. [PubMed: 20800680]
59. Milla P, Dosio F, Cattel L. PEGylation of proteins and liposomes: A powerful and flexible strategy to improve the drug delivery. Curr Drug Metab. 2012; 13:105. [PubMed: 21892917]
60. Kishimoto K, Altreuter D, Johnston L, Keller P, Pittet L. SEL-068 a fully synthetic nanoparticle vaccine for smoking cessation and relapse prevention. Society for Research on Nicotine and Tobacco's 18th Annual Meeting. 2012 Abstract Book. POS1-1.
61. Jegerlehner A, Tissot A, Lechner F, Sebbel P, Erdmann I, Kündig T, Bächi T, Storni T, Jennings G, Pumpens P, Renner WA, Bachmann MF. A molecular assembly system that renders antigens of choice highly repetitive for induction of protective B cell responses. Vaccine. 2002; 20:3104. [PubMed: 12163261]
62. Maurer P, Jennings GT, Willers J, Rohner F, Lindman Y, Roubicek K, Renner WA, Müller P, Bachmann MF. A therapeutic vaccine for nicotine dependence: Preclinical efficacy, and Phase I safety and immunogenicity. Eur J Immunol. 2005; 35:2031. [PubMed: 15971275]
63. Ambühl PM, Tissot AC, Fulurija A, Maurer P, Nussberger J, Sabat R, Nief V, Schellekens C, Sladko K, Roubicek K, Pfister T, Rettenbacher M, Volk HD, Wagner F, Müller P, Jennings GT, Bachmann MF. A vaccine for hypertension based on virus-like particles: Preclinical efficacy and phase I safety and immunogenicity. J Hypertens. 2007; 25:63. [PubMed: 17143175]
64. Kündig TM, Senti G, Schnetzler G, Wolf C, Prinz Vavricka BM, Fulurija A, Hennecke F, Sladko K, Jennings GT, Bachmann MF. Der p 1 peptide on virus-like particles is safe and highly immunogenic in healthy adults. J Allergy Clin Immunol. 2006; 117:1470. [PubMed: 16751015]
65. Cornuz J, Zwahlen S, Jungi WF, Cornuz J, Zwahlen S, Jungi WF, Osterwalder J, Klingler K, van Melle G, Bangala Y, Guessous I, Müller P, Willers J, Maurer P, Bachmann MF, Cerny TA. A vaccine against nicotine for smoking cessation: A randomized controlled trial. PLoS One. 2008; 3:e2547. [PubMed: 18575629]
66. Banerjee K, Klasse PJ, Sanders RW, Pereyra F, Michael E, Lu M, Walker BD, Moore JP. IgG subclass profiles in infected HIV type 1 controllers and chronic progressors and in uninfected recipients of Env vaccines. AIDS Res Hum Retroviruses. 2010; 26:445. [PubMed: 20377426]
67. Sokolovska A, Hem SL, HogenEsch H. Activation of dendritic cells and induction of CD4(+) T cell differentiation by aluminum-containing adjuvants. Vaccine. 2007; 25:4575. [PubMed: 17485153]
68. O'Hagan DT, Rappuoli R. Novel approaches to vaccine delivery. Pharm Res. 2004; 21:1519. [PubMed: 15497674]

Author Manuscript Author Manuscript Author Manuscript Author Manuscript

69. Rosenkrands I, Agger EM, Olsen AW, Korsholm KS, Andersen CS, Jensen KT, Andersen P. Cationic liposomes containing mycobacterial lipids: A new powerful Th1 adjuvant system. Infect Immun. 2005; 73:5817. [PubMed: 16113300]

70. Becker M, Reuter S, Friedrich P, Doener F, Michel A, Bopp T, Klein M, Schmitt E, Schild H, Radsak MP, Echtenacher B, Taube C, Stassen M. Genetic variation determines mast cell functions in experimental asthma. J Immunol. 2011; 186:7225. [PubMed: 21572035]

71. McNair E, Bryson R. Effects of nicotine on weight change and food consumption in rats. Pharmacol Biochem Behav. 1983; 18:341.

72. Grunberg NE, Winders SE, Popp KA. Sex differences in nicotine's effects on consummatory behavior and body weight in rats. Psychopharmacology (Berl). 1987; 91:221. [PubMed: 3107036]

73. Gross J, Stitzer ML, Maldonado J. Nicotine replacement: Effects of postcessation weight gain. J Consult Clin Psychol. 1989; 57:87. [PubMed: 2925978]

74. Nabors CE, Ball CR. Spontaneous calcification in hearts of DBA mice. Anat Rec. 1969; 164:153. [PubMed: 4181974]

75. Goto N, Kato H, Maeyama J, Shibano M, Saito T, Yamaguchi J, Yoshihara S. Local tissue irritating effects and adjuvant activities of calcium phosphate and aluminium hydroxide with different physical properties. Vaccine. 1997; 15:1364. [PubMed: 9302746]

76. Baylor NW, Egan W, Richman P. Aluminum salts in vaccines-US perspective. Vaccine. 2002; 20:S18. [PubMed: 12184360]

77. Lindblad EB. Aluminium adjuvants-in retrospect and prospect. Vaccine. 2004; 22:3658. [PubMed: 15315845]

78. Butler NR, Voyce MA, Burland WL, Hilton ML. Advantages of aluminium hydroxide adsorbed combined diphtheria, tetanus, and pertussis vaccines for the immunization of infants. Br Med J. 1969; 1:663. [PubMed: 5774314]

79. Frost L, Johansen P, Pedersen S, Veien N, Ostergaard PA, Nielsen MH. Persistent subcutaneous nodules in children hyposensitized with aluminium-containing allergen extracts. Allergy. 1985; 40:68.

80. White RG, Coons AH, Connolly JM. Studies on antibody production. III. The alum granuloma. J Exp Med. 1955; 102:73. [PubMed: 14392242]

81. Erdohazi M, Newman RL. Aluminium hydroxide granuloma. Br Med J. 1971; 3:621. [PubMed: 5569985]

82. Goto N, Akama K. Histopathological studies of reactions in mice injected with aluminum-adsorbed tetanus toxoid. Microbiol Immunol. 1982; 26:1121. [PubMed: 7169970]

Author Manuscript Author Manuscript Author Manuscript Author Manuscript

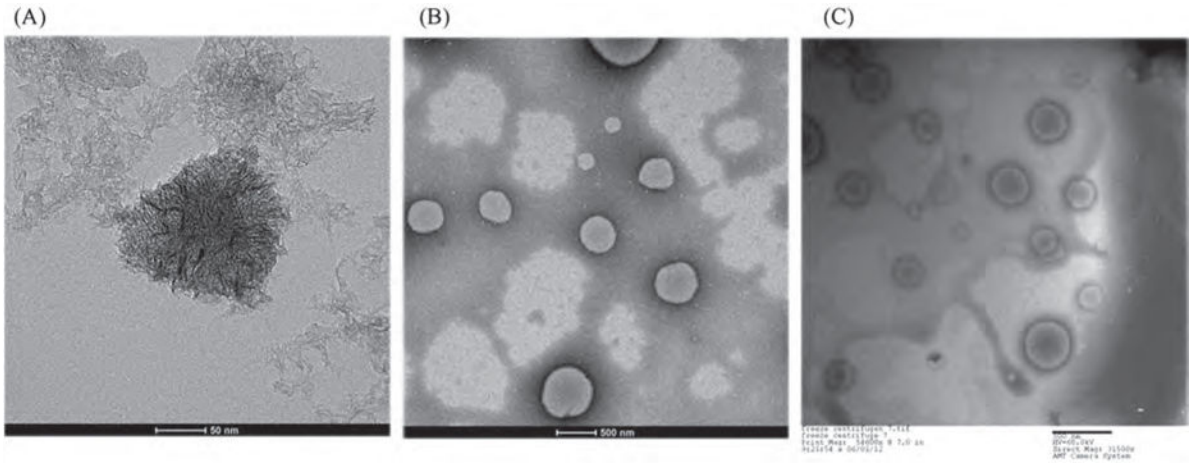

Figure 1.

TEM images of (A) nanohorn, (B) liposomes prepared with DOTAP, and (C) NsL. Scale bar in (A) = 50 nm. Scale bar in (B) and (C) = 500 nm.

Author Manuscript Author Manuscript Author Manuscript Author Manuscript

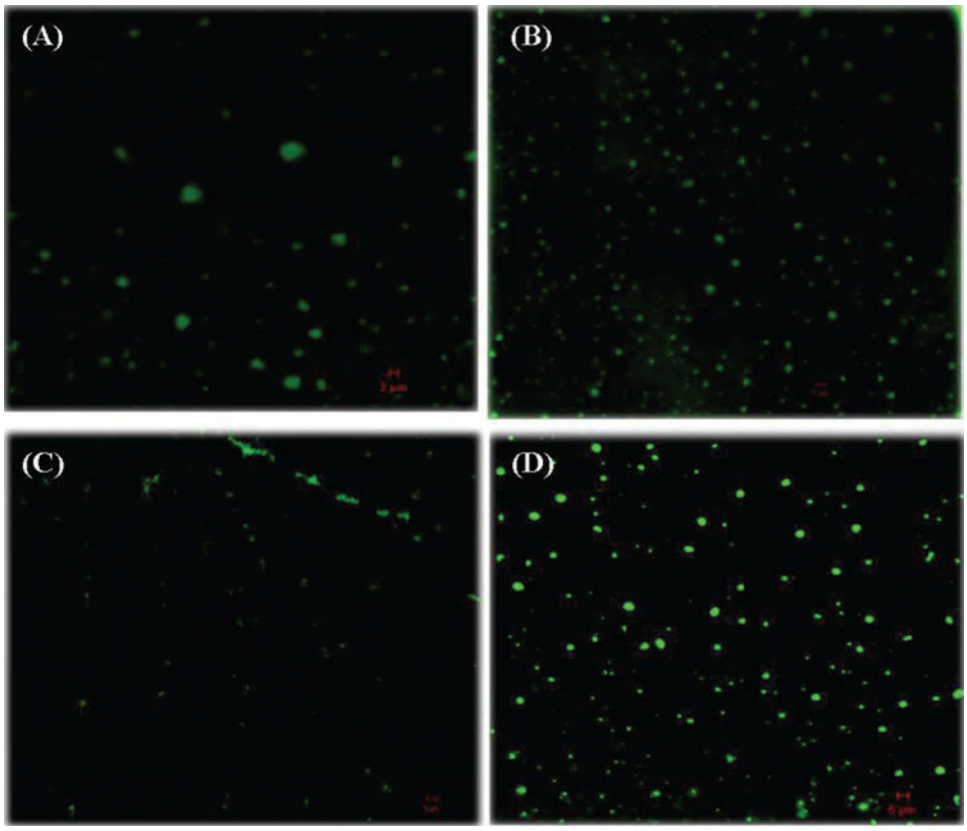

Figure 2.

Confocal microscopic images of liposomes and nanohorn supported liposomes labeled with FITC. (A) Newly synthesized liposomes, (B) newly synthesized nanohorn supported liposomes, (C) liposomes after storage for 5 days, (D) nanohorn supported liposomes after storage for 5 days.

Author Manuscript Author Manuscript Author Manuscript Author Manuscript

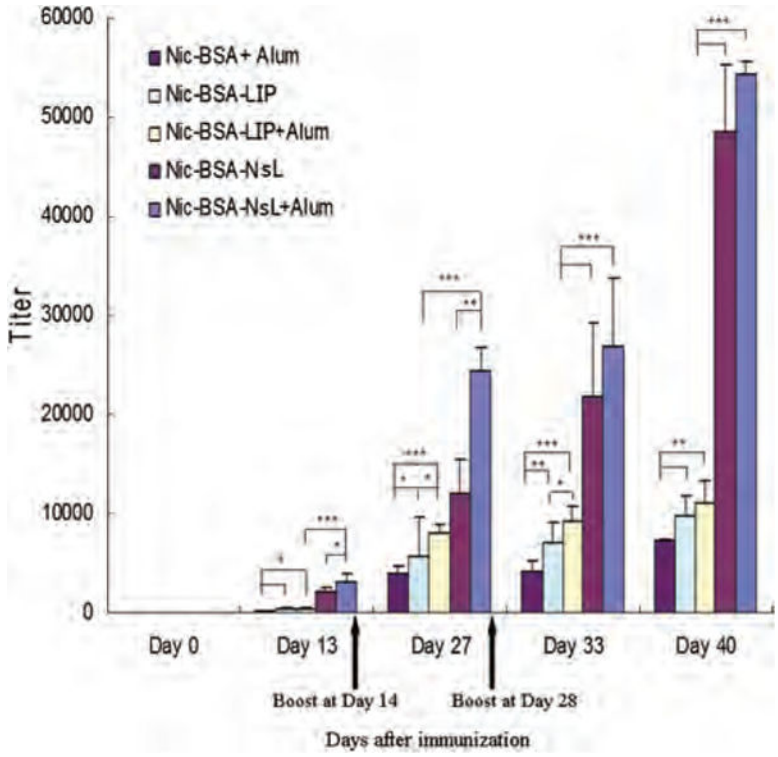

Figure 3.

Time-course of IgG nicotine-specific response to subcutaneous immunization with nicotine vaccines. Mice were given 50 μg of Nic-BSA with Alum and Nic-BSA-LIP or Nic-BSA-NsL with or without Alum adjuvant on days 0, 14 and 28. Two groups of control animals received either LIP with Alum or NsL with Alum, respectively. Serum samples from eight animals per group were taken at two weekly intervals. Control animals showed no detectable nicotine-specific IgG. Mean nicotine-specific serum IgG antibody titers and the corresponding standard deviations are represented by columns and error bars (*$P < 0.05$; **$P < 0.01$; ***$P < 0.001$).

Author Manuscript Author Manuscript Author Manuscript Author Manuscript

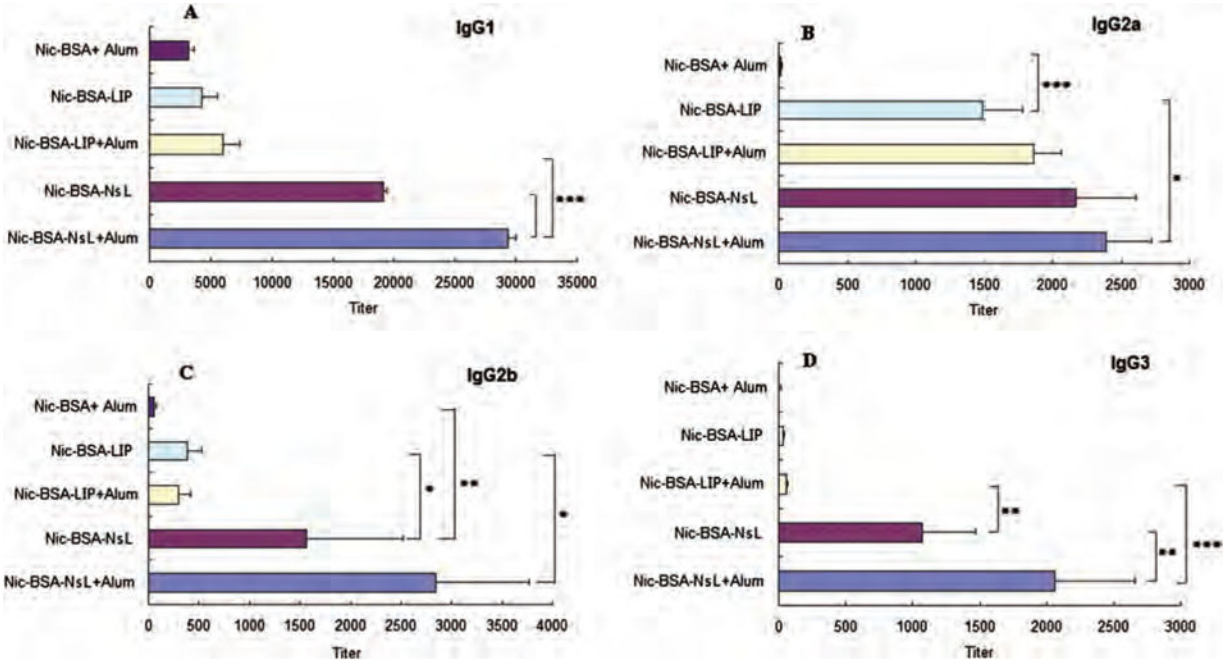

Figure 4.

Responses of IgG subclasses to subcutaneous immunization with nicotine vaccines. Mice were given 50 μg of Nic-BSA with Alum and Nic-BSA-LIP or Nic-BSA-NsL with or without Alum adjuvant on days 0, 14 and 28. Serum samples from eight animals per group were taken on day 40. Mean nicotine-specific serum IgG subclass antibody titers and the corresponding standard deviations are represented by columns and error bars (* $P < 0.05$; ** $P < 0.01$; *** $P < 0.001$).

Author Manuscript
Author Manuscript
Author Manuscript
Author Manuscript

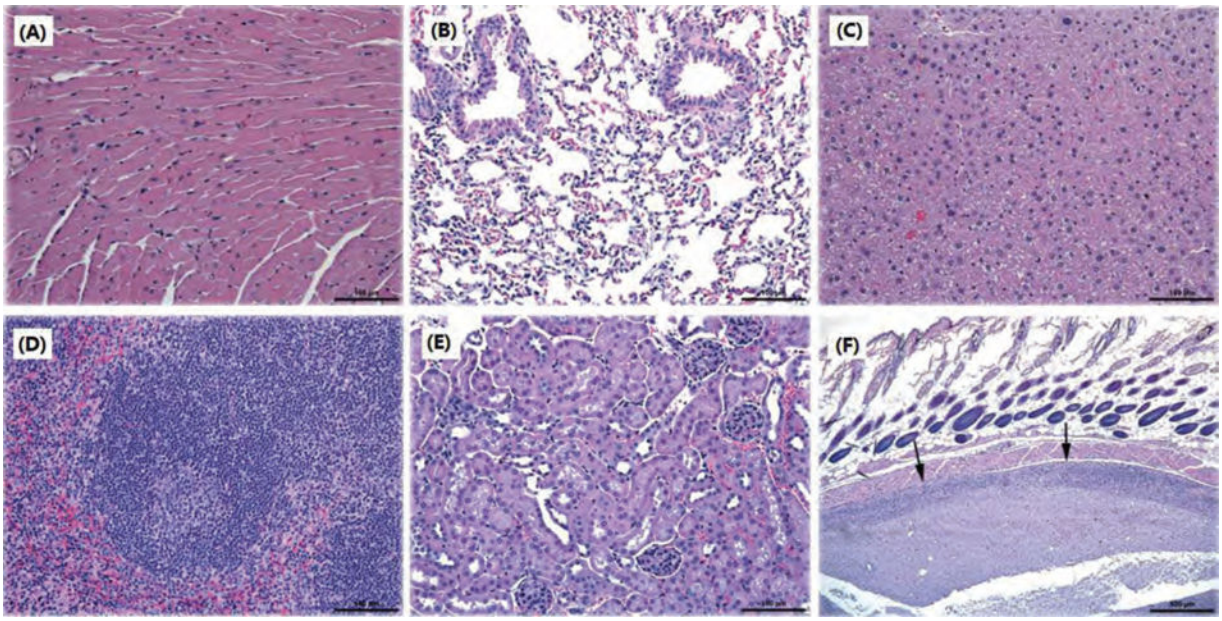

Figure 5.

Representative histopathological images of different mouse tissues after subcutaneous administration of nicotine vaccines. No lesions were noted in (A) heart, (B) lung, (C) liver, (D) spleen, and (E) kidney. (F) is from a mouse given a vaccine with Alum. Arrows indicate subcutaneous lesions. Scale bars in (A)–(E) are 100 μm; for (F) the scale bar is 500 μm.

Author Manuscript

Author Manuscript

Author Manuscript

Author Manuscript

Table I

Immunization scheme of mice (Balb/c). Each group had 8 mice. All vaccines (suspended in 100 μL saline) were administered subcutaneously with one primary immunization and two boosters two weeks apart.

Group no.	Vaccine name	Dose of immunogen (μg)	Dose of Alum (mg)
1	Nic-BSA	50	1.2
2	Nic-BSA-LIP	50	–
3	Nic-BSA-LIP	50	1.2
4	Nic-BSA-NsL	50	–
5	Nic-BSA-NsL	50	1.2
6	LIP	–	1.2
7	NsL	–	1.2

Notes: BSA: bovine serum albumin; LIP: liposome; NsL: nanohorn supported liposome.

Author Manuscript

Author Manuscript

Author Manuscript

Author Manuscript

Table II

Determination of Nic-hapten density, Nic-BSA thiolation grade and AE and LC of Nic-BSA to NsL NPs.

Molar ratio of additive (BSA: Nic:Traut's reagent: DSPE-Mal-PEG2000)	Approximate no. of amino groups used	Approximate no. of thiol groups used	AE (%)	LC (%)
1:50:200:4	15.1 (15)	5.69 (5)	50.4 ± 1.0	21.7 ± 2.4
1:50:200:8	15.1 (15)	5.69 (5)	65.8 ± 1.4	25.3 ± 4.6

Notes: Results are expressed as means (SD) for $n = 3$. AE: association efficiency; LC: loading capacity.

Author Manuscript

Author Manuscript

Author Manuscript

Author Manuscript

Table III

Size distribution and zeta potential of nanohorn, DOTAP liposomes, NsL and Nic-BSA-NsL in 0.15 M pH 7.4 NaCl solution or ultrapure water.

	Size (nm)	Zeta potential (mV)	Polydispersity
Nanohorn	107.8 ± 3.3	−29.5 ± 1.29	0.18 ± 0.02
DOTAP liposomes	152.0 ± 6.0	42.8 ± 0.96	0.20 ± 0.03
NsL	164.9 ± 2.5	47.6 ± 1.10	0.23 ±0.02
Nic-BSA-NsL	175.3 ± 3.2	52.2 ± 1.38	0.19 ± 0.01

Note: Results are expressed as means±SD *(n* = 3).

Author Manuscript Author Manuscript Author Manuscript Author Manuscript

Table IV

Th1:Th2 index for nicotine vaccine.

	Nic-BSA + Alum	Nic-BSA-LIP	Nic-BSA-LIP + Alum	Nic-BSA-NsL	Nic-BSA-NsL + Alum
IgG1 (Th2)	$(3.18 \pm 0.48)\times10^3$	$(4.25 \pm 1.32)\times10^3$	$(5.99 \pm 1.37)\times10^3$	$(1.91 \pm 0.03)\times10^4$	$(2.94 \pm 0.07)\times10^4$
IgG2a (Th1)	16.3 ± 4.5	$(1.49 \pm 0.29)\times10^3$	$(1.86 \pm 0.20)\times10^3$	$(2.17 \pm 0.45)\times10^3$	$(2.39 \pm 0.34)\times10^3$
IgG3 (Th1)	9.4 ± 4.2	32.4 ± 7.7	56.5 ± 6.5	$(1.57 \pm 0.96)\times10^3$	$(2.85 \pm 0.92)\times10^3$
Th1/Th2 index	0.004	0.180	0.160	0.085	0.076

Note: Results are expressed as mean±SD, $n = 8$.

Author Manuscript Author Manuscript Author Manuscript Author Manuscript

Table V

Effect of subcutaneous administration of nicotine vaccine on weight gains, feed consumption and water consumption of Balb/c mice.

	Body weight (g)			Food consumption (g/day)	Water consumption (g/day)
	Initial	Final	Change		
LIP + Alum	18.0 ± 1.6	20.9 ± 1.9	2.9 ± 0.6	2.8 ± 0.2	4.6 ± 0.5
NsL + Alum	17.9 ± 1.4	20.7 ± 1.7	2.8 ± 0.6	2.9 ± 0.2	4.3 ± 0.5
Nic- BSA + Alum	17.4 ± 0.7	20.4 ± 1.1	3.0 ± 0.7	2.6 ± 0.1	4.2 ± 0.5
Nic-BSA-NsL	18.4 ± 1.1	21.3 ± 1.5	2.9 ± 0.5	2.7 ± 0.3	4.4 ± 0.6
Nic-BSA-NsL + Alum	19.0 ± 0.9	21.7 ± 2.3	2.7 ± 1.7	2.8 ± 0.3	4.3 ± 0.7
Nic-BSA-LIP	17.9 ± 1.3	20.4 ± 1.6	2.5 ± 0.3	2.7 ± 0.4	4.6 ± 0.7
Nic-BSA-LIP + Alum	18.2 ± 1.4	21.0 ± 1.4	2.8 ± 0.9	2.7 ± 0.2	4.4 ± 0.6

Notes: Results of the mean body weight gains, feed consumption and water consumption of seven groups of mice are expressed as means ± SD. Data were analyzed by paired *t* tests and no differences were significant *(P* > 0.05, *n* = 8).

Author Manuscript Author Manuscript Author Manuscript Author Manuscript

Table VI

Effect of nicotine vaccines on body weight and organ/body weight ratio of Balb/c mice.

		Organ/Body weight ratios (%)				
Group	**Body weight (g)**	**Heart**	**Lung**	**Liver**	**Spleen**	**Kidney**
LIP + Alum	21.21 ± 1.70	0.66 ± 0.08	1.40 ± 0.53	5.11 ± 0.56	0.47 ± 0.08	1.47 ± 0.24
Nic-BSA + Alum	20.36 ± 1.29	0.65 ± 0.12	1.62 ± 0.27	5.02 ± 0.17	0.47 ± 0.07	1.53 ± 0.13
NsL + Alum	20.68 ± 1.73	0.74 ± 0.06	1.50 ± 0.26	5.17 ± 0.55	0.52 ± 0.07	1.54 ± 0.14
Nic-BSA-NsL	21.28 ± 1.52	0.74 ± 0.08	1.39 ± 0.22	5.28 ± 0.53	0.47 ± 0.06	1.53 ± 0.15
Nic-BSA-NsL + Alum	21.68 ± 2.27	0.75 ± 0.12	1.53 ± 0.35	5.25 ± 0.20	0.52 ± 0.04	1.56 ± 0.26
Nic-BSA-LIP	20.43 ± 1.58	0.65 ± 0.13	1.59 ± 0.41	4.92 ± 0.39	0.46 ± 0.05	1.51 ± 0.18
Nic-BSA-LIP + Alum	21.03 ± 1.37	0.74 ± 0.14	1.60 ± 0.27	4.85 ± 0.30	0.50 ± 0.08	1.49 ± 0.15

Notes: Results of the mean body weight and organ/body weight ratio of seven groups mice are expressed as means±SD. Data were analyzed by paired *t* tests and no differences were significant ($P > 0.05$, $n = 8$).